ISSN 1023-1935, Russian Journal of Electrochemistry, 2016, Vol. 52, No. 9, pp. 910–919. © Pleiades Publishing, Ltd., 2016.
Original Russian Text © S.V. Shevkunov, 2016, published in Elektrokhimiya, 2016, Vol. 52, No. 9, pp. 1022–1032.

Structure and Electric Properties of Sodium Ion Hydrate Shell in Nanopore with Hydrophilic Walls[1]

S. V. Shevkunov

Peter the Great St. Petersburg State Polytechnical University, ul. Politekhnicheskaya 29, 195251 St. Petersburg, Russia
e-mail: shevk54@mail.ru

Received October 20, 2015

Abstract—The method of molecular–level computer simulation at the temperature of 298 K was used to study the fundamental regularities of formation of electric properties of the hydrate shell of the Na^+ cation in a planar model nanopore with hydrophilic structureless walls in contact with water vapors. Electric polarizability changes nonmonotonously: as consistent with the changes in the molecular structure of the system. Hydration within the pore occurs in several stages, from formation of chain structures, microdrop compaction and ejection of the ion from its own hydrate shell to encapsulation and absorption of the ion by the solvent preceding formation of nanoelectrolyte. Despite the significant differences in the energy of retaining hydrate shells for Na^+ and Cl^- ions, polarizabilities of the two systems are close and behave similarly under variation of conditions. Strong spatial anisotropy of the polarizability tensor of the ion–hydrate complex is due to the effect of the nanopore walls on multiparticle spatial correlations in the system.

Keywords: hydration, ions, nanopores, computer simulation, electric polarizability

DOI: 10.1134/S1023193516090093

1. INTRODUCTION

Hydration of ions in nanosized volumes is of theoretical interest for adsorption mechanisms on nonideal surfaces [1], metal corrosion [2], diffusion of ions through membranes [3], and heterogeneous nucleation of atmospheric moisture on aerosol particles with active centers [4]. High efficiency of chemical power sources [5], electric batteries [6, 7], fuel cells [8], and electrochemical capacitors [9–11] depends on the contact area between electrolyte and the electrode surface [12]. An increase in the area is provided by using surfaces with a nonuniform porous structure [13, 14]. A decrease in the pore size causes an increase in the effective contact area. At the same time, the behavior of hydrated charges in nanosized cavities may be fundamentally different for their properties in bulk materials [15].

Difficulties of analytical description render the theory of nanoelectrolytes and hydrated charges on the nanoscale an insufficiently developed area. Under the conditions when the system dimensions are comparable with the radius of intermolecular correlations, application of mean field theory approximations and especially continuous medium theory approximations is impossible. At the same time, due to the extraordinary computational problems achieving also a strict quantitative statistic–mechanical description with a successive calculation of the partition function and equilibrium mean values appears unrealistic. Despite the nanosize, such systems may contain too many particles for comprehensive analytical calculations.

An effective research instrument here is computer simulation at the molecular level [16]. High efficiency of stochastic methods in systems with a large number of particles is due to using the random sampling tool. A weak point of the method is the numeric form of the obtained results and large amount of calculation corresponding to hundreds of hours of computer time.

In [17–19], the Monte Carlo method is used to study structural and thermodynamic properties of a hydrated Cl^- ion under the conditions of a nanoscopic pore with structureless hydrophobic walls. In [20, 21], similar studies were carried out for the Na^+ cation. In [22], structural and electric properties of a hydrate shell of the Cl^- anion were studied in a nanopore with structureless hydrophilic walls. This work studies the regularities of formation of electric and structural properties of water microdroplets growing at the room temperature in the field of a Na^+ cation under the conditions of a planar molecular nanosized pore with hydrophilic structureless walls, as in [22]. The aim of the work is to study universal regularities unrelated to any specific wall surface properties.

[1] The paper is dedicated to the memory of academician V.A. Kistyakovskii (1865–1952).

2. RESULTS OF COMPUTER SIMULATION

The simulation parameters are similar to those used in [22]. The computer calculations using the Monte Carlo method are performed for planar pores with the width of 0.7 and 1.0 nm. Attraction of molecules to the walls is described by one–dimensional rectangular potential. The potential well width of 0.1 nm is close to the value of the corresponding minimum in the potential of intermolecular interactions.

The sodium ion Na^+ is fixed in the center between the pore walls and the molecules can move freely within the pore in the space confined in a sphere with the radius of 2 nm around the ion. No periodical boundary conditions are applied. The equilibrium characteristics are obtained by averaging over $\approx 2\times10^8$ configurations. Before calculations of the mean values, the system is brought into the thermodynamic equilibrium. The length of the thermalization segment is 5×10^7 Markov moves.

The description of intermolecular interactions and interactions with the ions is carried out especially thoroughly by using an extended many-body interaction potential ICP(SPC) (Ions + Covalent bonds + Polarization based on SPC geometry) calibrated on the basis of experimental data for free energy and enthalpy of hydration of the ion in water vapors [23, 24] and tested in modeling of the bulk aqueous electrolyte [25] and ionization in clusters of water molecules [26, 27]. The free energy and entropy of the addition reactions are calculated using the bicanonical ensemble method (BEM) [19, 28–30]. Apart from the pair coulombic and exchange interactions, the model also includes nonpair polarization interactions and covalent interaction and accounts for the effects of excessive charge transfer to molecules and interactions with induced dipoles. It explicitly accounts for polarization of the molecules in the field of the ion and polarization of the ion in the field of the molecules. Numeric values of the model parameters were determined on the basis of the conditions of adjustment of the calculated and experimental values of free energy and enthalpy of the first reactions of vapor molecules attachment to the ion [31] and also reproducibility of the geometric parameters in locally stable configurations of molecular clusters obtained in quantum–chemical calculations [32]. Calculations of the equilibrium states are carried out at temperature $T = 298$ K for three values of the potential well depth: 2.5, 5.0, and 10 k_BT.

a. Mechanism of Hydrate Shell Retention

The experimental values of free energy of attachment reactions in bulk water vapors to sodium cation $Na^+(H_2O)_{n-1} + H_2O \rightarrow Na^+(H_2O)_n$ [31] and chloride anion $Cl^-(H_2O)_{n-1} + H_2O \rightarrow Cl^-(H_2O)_n$ [33] differ considerably. The free energy of the first reaction ($n = 1$) in the case of the sodium cation is 15 k_BT lower than for the chloride anion. In the further reactions, the difference decreases, but remains significant: 11, 7, and 4 k_BT.

A stronger bond with the molecules closest to the sodium cation is explained by two factors: the smaller ion size and asymmetry of electric charge location in the water molecule. The positively charged sodium cation is bound to the water molecule through its oxygen atom with its excessive negative charge, while the negatively charged chloride anion is bound to one of the hydrogen atoms of the molecule. The oxygen atom of the water molecule bears a twice higher absolute charge as compared to the hydrogen atom. This explains the stronger electrostatic interaction in the case of the sodium cation.

The advantage of the sodium ion with respect to electrostatic retention of the closest molecules proves to be a more significant factor than the circumstance that a water molecule can play a role of hydrogen bond donor for the chloride–containing anion. High polarizability of the chloride anion in the aqueous medium (3.59 Å^3) as compared to the sodium cation (0.079 Å^3) and therefore high mobility of the electron shell also prove to be an insufficiently strong argument to shift the balance towards the chloride ion.

A string bond between the first four attached molecules and the sodium cation provides relative strength of the hydrate shell only at the initial stage of formation. The attachment of the further molecules directly to the ion is hindered due to two circumstances: due to the effect of saturation of bonds with the ion caused by excitations in the outer electron shells and the unfavorable entropic factor related to contraction of the free space near the ion. The effects of bond saturation cannot be described within the simplest pair interaction model. The ICP(SPC) model of intermolecular interactions accounts for nonpair interactions of both polarization and covalent type. The role of nonpair interactions in the hydrate shell of a sodium ion in the bulk phase is studied in detail in [34]; that in the hydrate shell of the chloride ion is described in [35, 36].

The effect of the above factors at an increase in the number of molecules retained in the field of the ion results in thermodynamic unfavorability of the attachment directly to the ion. The following added molecules are retained not due to direct interactions with the ion, but due to hydrogen bond formed with the molecules attached earlier, i.e, molecular chains are formed, as in Figs. 1a, 1b, that tend to close into molecular cycles with four to six links at an increase in the system size, Figs. 1b, 1c. The closing trend is counteracted by two factors: electrostatic repulsion of chains with strong electric polarization and unfavorable entropy of transformation of loose chain structure into more compact ones. The effect of repulsion of

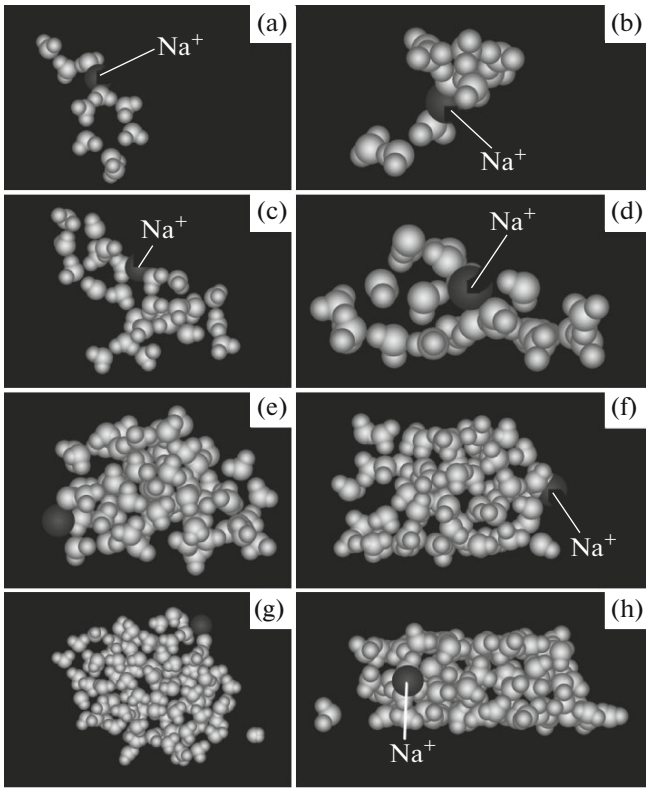

Fig. 1. Hydration of the Na^+ ion fixed between the hydrophilic walls in a planar nanopore with the width of 0.7 nm in water vapors at the temperature of 298 K. The width of the potential well near the walls is 0.1 nm, adsorption energy on the walls is 2.5 k_BT. (a, c, e, g) Appearance in the direction perpendicular to the pore plane, (b, d, f, h) appearance along the pore plane.

polarized molecular chains in a strong electric field is studied in detail in [37, 38].

b. Ion Encapsulation and Formation of Nanoelectrolyte

The further increase in the amount of molecules near the ion is accompanied by a decrease in the available configuration space and thus a decrease in entropy. The energy favorability of chain closing prevails and the space inside the pore is filled by molecules forming a compact clot, Figs. 1d–1h. At this stage, the effect of ion displacement from its own hydrate shell becomes pronounced. The effect of ions displacement first observed in bulk water vapors for the chloride anion [35, 39–42], was later reproduced under the same conditions for the sodium cation [34]. Detailed analysis of the causes of this phenomenon can be found in [17, 43].

Full ion encapsulation by molecules is absent here even in a cluster consisting of 100 molecules. At the same time it is obvious that encapsulation occurs in the system of sufficiently large size. This follows from the unfavorable entropy factor on the surface of a sufficiently large drop. In a system unrestricted by a planar pore, an increase in the size brings about an increase in the system volume as a cube of its linear dimensions, while the surface layer volume grows proportionally to a square of its linear dimensions. The same behavior is observed for the corresponding configuration spaces. Under the conditions of a planar nanopore, the system volume grows square–law and the volume of the peripheral layer is proportional to the linear dimensions. Though the growth rates here are different, the relationship between them remains qualitatively the same as in the bulk system.

One should expect ion encapsulation in a nanopore after a certain critical amount of molecules is exceeded. In fact, at this moment, the ion is absorbed by the solvent and a nanoelectrolyte as such is formed. Formation of a nanoelectrolyte in a nanopore by absorption of water vapors and growth of a molecular clot hydrating the ion occurs only after a sufficient amount of water is accumulated.

c. Effect of Ion Displacement and Electric Properties

One should expect an increase in electric polarizability of the system on the whole due to ion displacement from the hydrate shell. This natural ion "hydrophobicity" with respect to its own hydrate shell causes transport of a part of molecules to greater distances, the weakening of the consolidating effect of the electric field of the ion, an increase in rotational mobility of molecules and thus an increase in polarizability.

The location of the ion on the molecular cluster surface increases the probability of direct interactions with both the other chemical impurities and the pore walls. The energetically favorable location of molecules in the field of an iron pair is between the ions [26, 27, 44, 45]. In such a configuration, the molecular cluster screens the electric field of ions and thus produces a containing effect on recombination. At the same time, there is a possibility for neutral molecules to form chemical bonds with the hydrated ion on the side free from water molecules. One can expect that this circumstance under the conditions of hydration must enhance the chemical activity of the ion.

In a pore with strongly hydrophilic walls, molecular chains are completely glued to the walls already at the early stage of hydration (Figs. 2a, 2b). The hydrate shell of the ion proves to be almost completely absorbed on the walls (Figs. 2c–2f). At the next stage, localization of all molecules on one of the walls appears to be more thermodynamically favorable (Figs. 2g, 2h), and not their distribution in fractions on the opposite walls. The appearance in the direction perpendicular to the pore plane (Figs. 2e, 2g) allows observing formation of molecular films spots on the walls. The structural elements of the film are long molecular chains. The coherent chains form cycles,

of which some reach the length of up to eight links (Fig. 2g).

The filling of the inner pore region by molecules under the conditions of strongly hydrophilic walls occurs later (at the greater amount of molecules drawn in), as compared to the conditions of weak hydrophilicity. Under the conditions of an extremely narrow pore (0.7 nm) with strongly hydrophilic walls, practically all water molecules turn out to be on the walls (Fig. 2). In a wider pore (1 nm) with moderately hydrophilic walls (Fig. 3), one can identify molecules playing the role of a binder between the ion and film on the walls.

At the stage when the molecules in the ion hydrate shell are present on the both walls, their relative shift is observed (Fig. 3d) due to the mutual repulsion owing to strong counter polarization in the field of the ion. The electric field of the ion retains repulsing spots and thus provides cohesiveness of the whole structure. Here, the ion is located over the spot edges playing the role of a "buckle". After all molecules move to one of the walls, the ion is located over the central region of the spot (Figs. 3g, 3h).

d. Electric Polarizability

Transformations in the form of a hydrate shell of the ion under the conditions of a pore cannot fail to reflect on its electric properties. It is natural to expect that the loose structure must promote enhanced system polarization and vice versa. The effect of collective effects due to strong spatial correlations of molecules can hardly be predicted on the basis of barely speculative grounds. This requires a detailed calculation.

Nondiagonal components of the electric polarizability tensor in the system of coordinates unrelated to the ion center and one of its axes (z) oriented normally to the pore plane are identically equal to zero due to the symmetry of the system. Diagonal tensor components α_x, α_y, α_z were calculated on the basis of the fluctuation theorem [46]. With account for the spatial symmetry of the system, $\langle P_x \rangle_c = 0$ and $\alpha_x = \langle P_x^2 \rangle_c / k_B T$. Here, P_x is the x-component of the dipole moment of the system in the system of coordinates related to the ion and brackets denote the canonical averaging. Similar formulas are true for the other two components.

Figure 4 shows the dependence on the amount of molecules in the system of specific lateral (in the direction of the pore plane) $\alpha_{\parallel} = (\alpha_x + \alpha_y)/2N$ and specific transverse (in the direction across the pore) $\alpha_{\perp} = \alpha_z / N$ electric polarizability of the hydrate shell of the Na^+ ion in the nanopore. Different curves were obtained in pores with different degrees of hydrophilicity of the walls. The pore drastically affects the electric polarizability of the system making it strongly anisotropic. Lateral polarizability (Fig. 4a) is on the

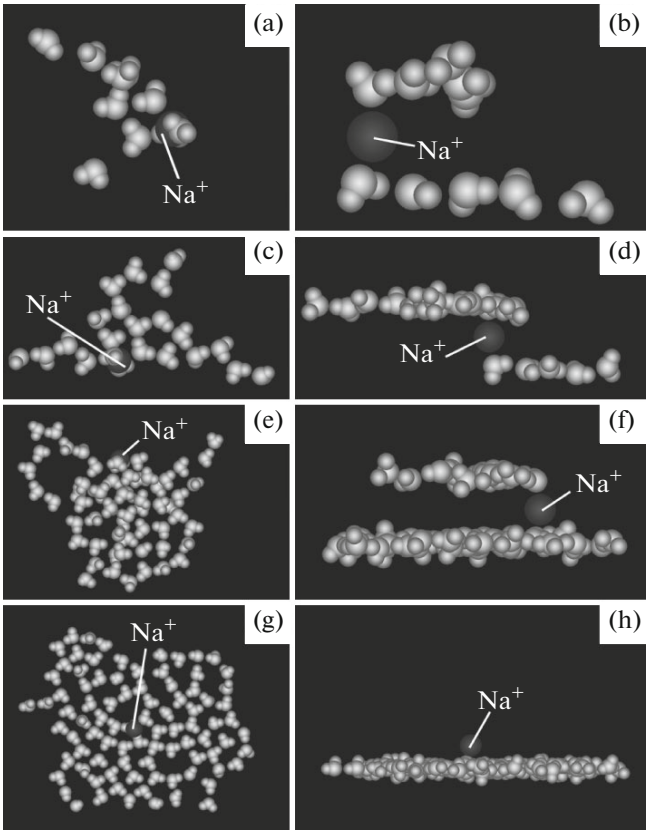

Fig. 2. The same as in Fig 1, in the pore with adsorption energy on the walls equal to 10 $k_B T$.

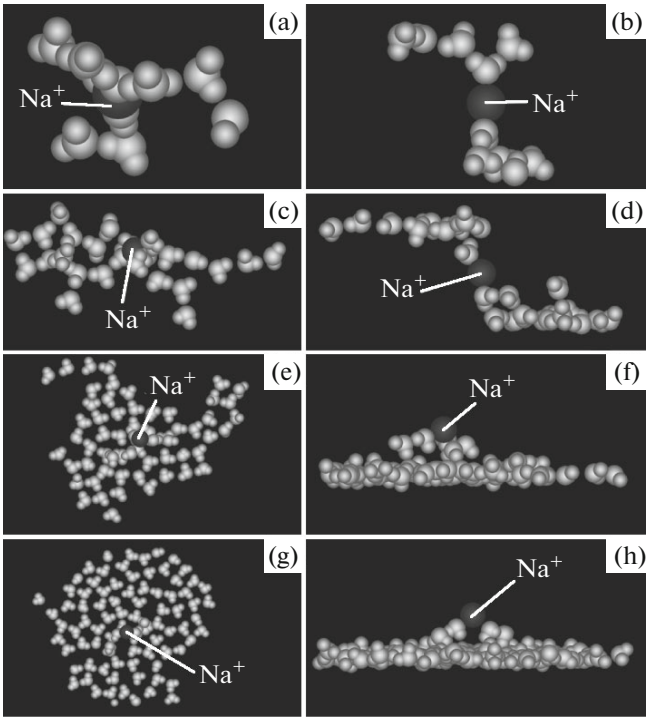

Fig. 3. The same as in Fig 1, in a 1 nm wide pore with the adsorption energy on the walls equal to 5 $k_B T$.

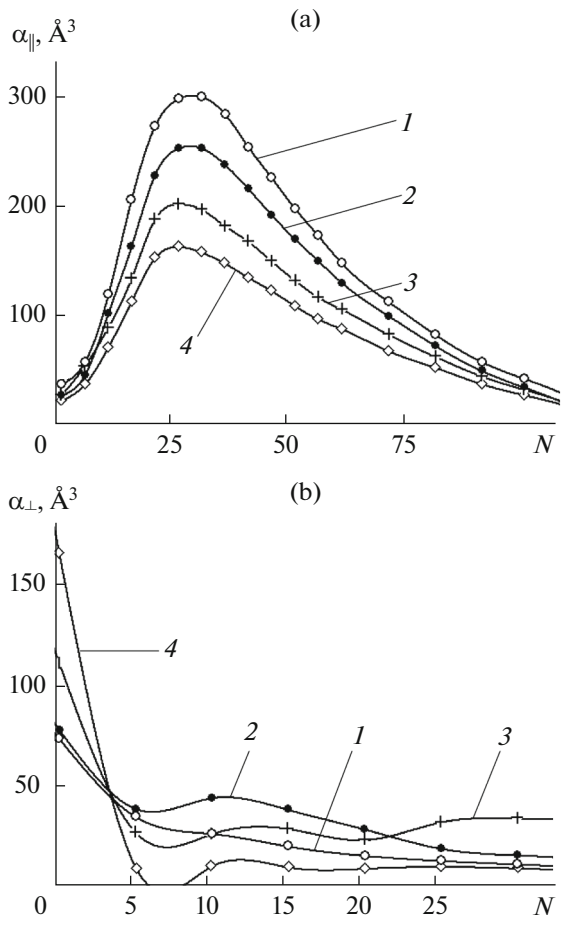

Fig. 4. Evolution of (a) lateral $\alpha_{\parallel}$ and (b) transverse $\alpha_{\perp}$ polarizability of the hydrate shell of the Na^+ ion per single molecule in a 0.7 nm wide planar nanopore with hydrophilic walls at the temperature of 298 K with an increase in the amount of molecules in the system. The adsorption energy on the walls: (*1*) 0.0, (*2*) 2.5, (*3*) 5.0, (*4*) 10 k_BT.

average higher than the transverse one (Fig. 4b) and demonstrates a qualitatively different behavior at an increase in the system size. If transverse polarizability, after an initial drastic decrease at the start of the curve, manifests relatively weak irregular variations around the values of 20–30 Å^3, the curve for the lateral component has a bell-like shape with a pronounced maximum at about $N \approx 25$.

Enhancement of hydrophilicity of the walls results in a decrease in the lateral polarizability component, while it is difficult to make a conclusive statement as to the direction of variation of the transverse component as dependent on the wall hydrophilicity against variations with the change in the system size. The maximum value of the lateral component exceeds 300 Å^3, which is two orders of magnitude higher that the intrinsic (electron) polarizability of a water molecule; it is achieved under the conditions of hydrophobic walls. Qualitatively, the behavior of polarizability of the hydrate shell of the Na^+ cation in the pore is similar to other dependences obtained for the Cl^- anion. The dependences are also close quantitatively, despite the difference both in the energy characteristics and in the molecular structure.

It comes to attention that the maximum of the lateral electric polarizability corresponds to the size, at which the hydrate shell in the bulk water vapors and in a pore with hydrophobic walls loses thermodynamic stability. This phenomenon is denoted in [34] as a "stability crisis". The stability crisis is characterized by an inflection point in the dependence of free energy on the size and is a boundary between the concave and convex curve regions. The phenomenon of stability loss is eliminated at an increase in the wall hydrophilicity and the hydrate shell turns out to be stable in the whole size range.

It is remarkable that the bell-like shape of the polarizability dependence with a characteristic maximum is preserved even when the effect of stability loss disappears completely, which occurs in a nanopore with strongly hydrophilic walls. Electric characteristics here manifest much higher sensitivity to transformations in the molecular structure than free energy. This phenomenon can be explained as follows. Stability loss of the system occurs simultaneously and is related to ion displacement from its own hydrate shell [34]. The ion is found on the molecular cluster surface and strongly polarizes it by its electric field, which is inevitably accompanied by a drastic increase in the overall dipole moment of the system. Obviously, exposure to an external electric field at the stability boundary must stimulate the above transformation with a drastic increase in the dipole moment. But this also means high electric polarizability manifesting itself in a pronounced maximum in Fig. 4a.

Enhanced polarizability means the growth of attraction forces of the hydrated ion to the sources of nonuniform electric field within the pore. Such sources can be both point crystalline defects on the walls and impurity ions within the pore. Enhanced polarizability of hydrate shells at the hydration stage corresponding to the maximum in Fig. 4a promotes cohesion of hydrated charges. Walls with a high degree of hydrophilicity suppress this effect.

e. 3D Organization

While instantaneous images (Figs. 1–3) hardly allow identifying any stable order in the spatial distribution of molecules, averaging by configurations allows educing a regular density distribution against the fluctuations, which points to its strong nonuniformity. In the near–wall layer (Fig. 5a), the density of molecules under the conditions of hydrophobic walls is small and does not exceed 20% of the density of water under normal conditions. Under the conditions of the intermediate degree of hydrophilicity, the den-

sity near the wall approaches the density of water, but the distribution remains sufficiently uniform. Under the conditions of intermediate (curve *3*) and strong (curve *4*) hydrophilicity, maximums and minimums are formed in the radial distribution, which points to the presence of strong spatial correlations between molecules. The density distribution near the wall has the shape of concentric rings encompassing a normal from the ion center to the wall. The first maximum in curve *4* in point $R = 0$ points to compaction in the near–wall layer directly under the ion. The presence of clearly pronounced maximums and minimums in curve *4* points to the high degree of structuring in the monomolecular film spot formed on the pore wall under the ion.

In the range located farther from the wall (Fig. 5b), the arrangement of curves *1–4* is opposite: the density of molecules in the range between the ion and the wall decreases at an increase in the surface hydrophilicity. The density in the layer in which the ion is located changed in the same direction (Fig. 5c). The relative arrangement of curves *1–4* along the vertical axis gives an idea how fast the hydrate shell of the ion is adsorbed on the walls. As opposed to the distributions in the subsurface layer (Fig. 5a), the maximums in Fig. 5c are not shifted at variation of hydrophilicity, but only their height is changed. Hence one can conclude that multiparticle intermolecular correlations being most sensitive towards the density produce a more considerable effect on the molecular order in the near–wall region than near the ion.

Dynamics of development of the molecular order in the system at the further stages of ion hydration are characterized by a faster growth of density of molecules in the near–wall layer (Fig. 6a), with the simultaneous slower accumulation of molecules in the gap between the ion and the wall (Fig. 6b) and also near the ion (Fig. 6c). The local density in the near–wall region can exceed the density of water under normal conditions (curves *3*, *4* in Fig. 6a), besides the spot structure at the final stages remains unchanged: in the middle, directly under the ion, an about 0.3 nm wide high–density region is formed, around which ring-shaped compaction regions are located. Comparison with similar 3D distributions in the field of the Cl^- anion points that not a density maximum, as in the case of the Na^+ cation, but a minimum is formed on the wall, directly under the chloride ion. The difference is explained by asymmetry of arrangement of electric charges with respect to the center of mass of the water molecule.

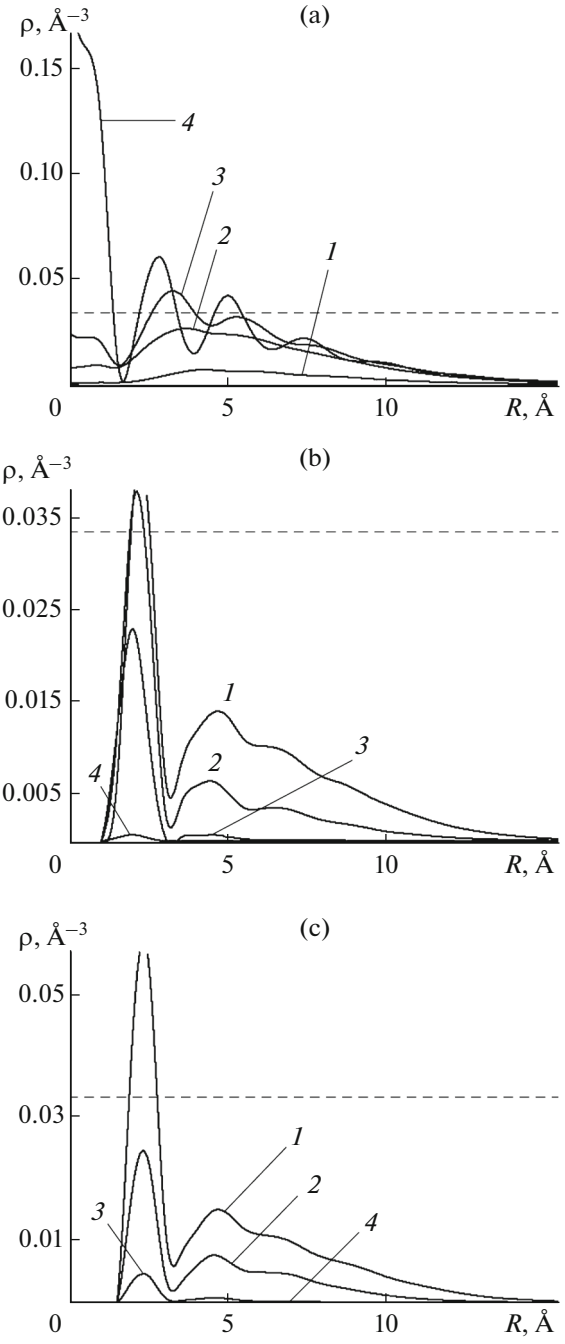

Fig. 5. Radial distributions of local density of 20 water molecules at the temperature of 298 K in the field of a Na^+ ion fixed between the walls of a 0.7 nm wide planar pore in parallel sections at different distances from the wall: (a) 0.05 nm; (b) 0.25 nm; (c) 0.35 nm. The adsorption energy on the walls: (*1*) 0.0, (*2*) 2.5, (*3*) 5.0, (*4*) 10 k_BT. Distance R is calculated from the normal from the pore plane passing through the ion center. The dashed line corresponds to the bulk density of water under normal conditions.

f. Orientational Order

The orientation molecular order is of considerable interest for electric properties. Figure 7 shows the angle distributions between the normal to the wall and vectors of dipole moments of water molecules. The molecules in the subsurface layer immediately adjacent to the wall are predominantly oriented so that their hydrogen atoms face the wall. This is supported by the maximums of distributions in Fig. 7a shifted

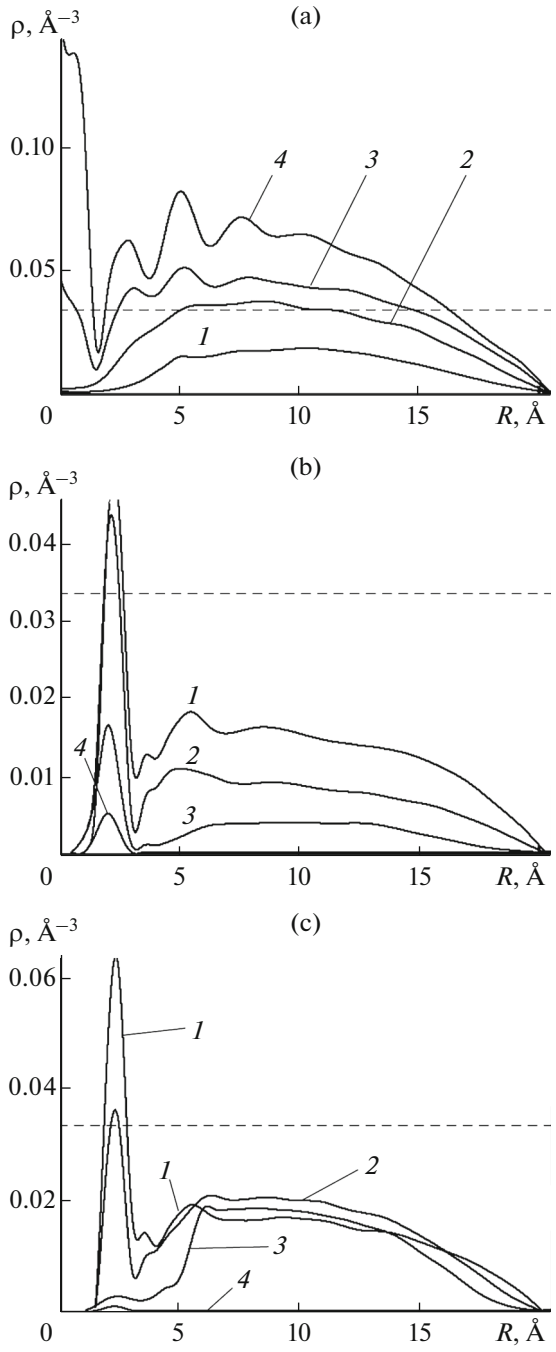

Fig. 6. The same as in Fig 5, for $N = 100$ molecules.

towards larger angles. Such orientation in the field of the positively charged ion appears to be quite natural. The deviation in the position of maximums from angle π corresponding to the orientation strictly in the normal direction to the wall is due to orientation of force lines of the electric field of the ion. To the accuracy of inverse orientation of force lines, the orientational order of the Na^+ ion near the wall is close to the orientational order under similar conditions in the field of the Cl^- ion (see Fig. 7a in [22]). The dependence of the orientational order near the wall on its hydrophilicity degree is weak in both cases.

A strong dependence of molecule orientations on the hydrophilicity degree of the walls is observed in the layers located approximately in the middle between the ion and the wall (Fig. 7b). Here, enhancement in hydrophilicity is accompanied by enhancement of polarization and more rigid orientation of molecules with their dipole moments towards the wall (compare curves *1*–*4*). The difference in the behavior of molecules in this region in the field of the Na^+ ion on the behavior of the field of the Cl^- ion (see Fig. 7b in [22]), to the accuracy of reorientation of dipole moments of molecules in accordance with the opposite direction of force lines of the electric field of the ion, consists in deviation of the maximum of distributions in the case of the negative ion from the orientation strictly along the normal to the wall. This deviation is due to the fact that hydrogen atoms bearing a positive change in the water molecule are not located on the symmetry axis of the molecule. At such distances from the ion, the significant effect on the orientational order is produced by higher multipole moments of the molecule.

In the range between the pore walls, the equilibrium angle distribution with respect to the point of $\theta = \pi/2$ must be symmetrical. As seen in Fig. 7c, the symmetry is present in the mode of hydrophobic walls and walls with weak hydrophilicity (curves *1*, *2*). Distortion of symmetry under the conditions of the intermediate and strong hydrophilicity (curves *3*, *4*) points to the presence of metastable states with an asymmetric distribution of molecules on the opposite walls. Stability of metastable states depends on collective effects and drops at a decrease in the amount of molecules in the system: angle distributions at the early hydration stage remain symmetrical under the conditions with different wall hydrophilicity degrees (curves *4* in Figs. 8a–8c).

The main transformations in the molecular order of the system at an increase in the wall hydrophilicity occur in the region roughly about the middle between the ion and the wall. The maximums of distributions here become more sharp (compare the shape of curves *2*, *3*, *5*, *6* in Figs. 8a–8c). This points to enhancement of the orientational order. Here, the angle distributions on the wall surface (curves *1*, *7*) and in the central pore region (curve *4*) change slightly.

The observed regularities in the transformation of the orientational order allow explaining a decrease in electric polarizability at an increase in hydrophilicity of the walls that can be seem in Fig. 4a (compare the positions of curves *1*–*4*). A decrease in polarizability occurs due to the stiffening of the orientational order in the region between the ion and the wall: fluctuations of angle θ decrease, rotation of the dipole moments towards the normal to the pore plane under

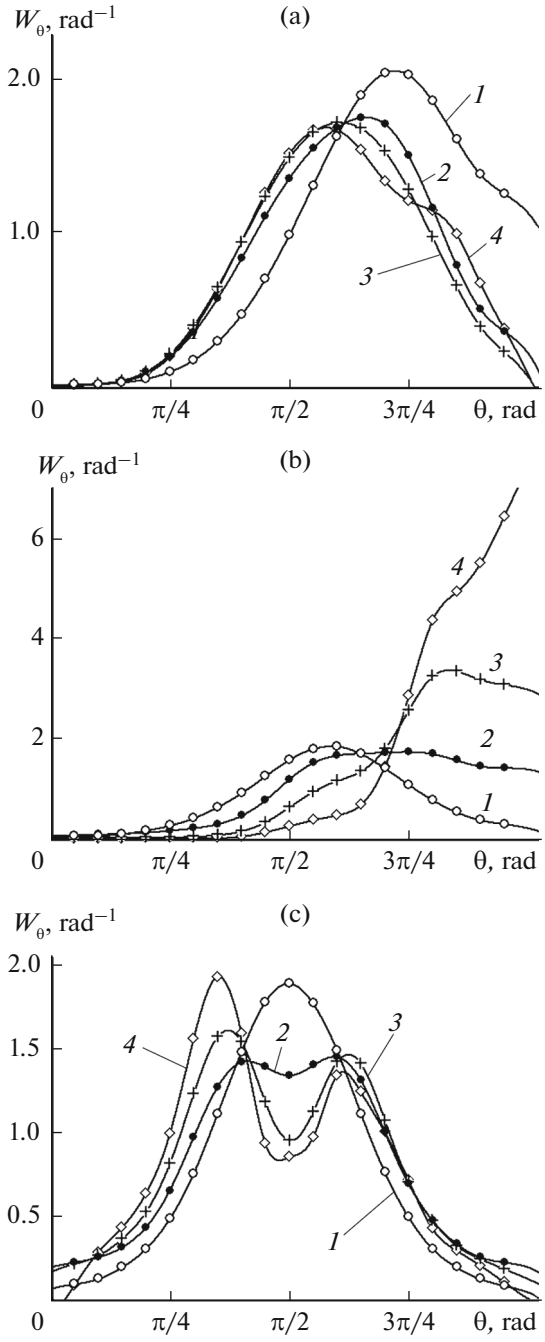

Fig. 7. Distributions by angle θ between the normal to the wall and the proper dipole moments for $N = 20$ water molecules in the field of the Na^+ ion fixed between hydrophilic pore walls with the width of 0.7 nm, at 298 K, at different distances from the wall: (a) 0.05 nm; (b) 0.25 nm; (c) 0.35 nm. Energy of adhesion of molecules to walls: (*1*) 0.0, (*2*) 2.5, (*3*) 5.0, (*4*) 10 k_BT.

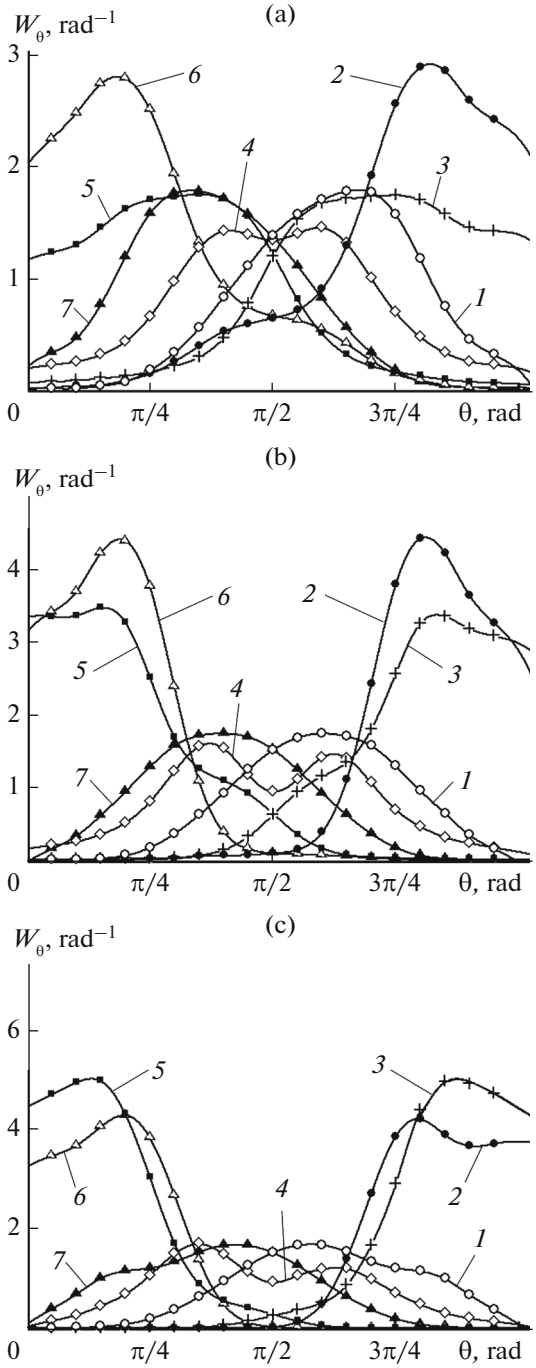

Fig. 8. The same angle distributions for $N = 10$ molecules under the conditions of different adsorption energy on the walls: (a) 2.5 k_BT, (b) 5 k_BT, (c) 10 k_BT. Distances from the wall, nm: (*1*) 0.05, (*2*) 0.15, (*3*) 0.25, (*4*) 0.35, (*5*) 0.45, (*6*) 0.55, (*7*) 0.65.

these conditions requires applying a stronger external electric field.

A decrease in specific polarizability at an increase in the number of molecules in the system to the right of the maximum in Fig. 4a (at $N > 25$) is related to the filling of the region between the ion and walls. The molecules in this region are most rigidly oriented. The fraction of these molecules at the intermediate hydration stage increases and their low rotation mobility provides the growing contribution into the decrease in the overall specific polarizability of the system.

Low transverse polarizability, as compared to lateral polarizability, as follows from comparison of locations of the curves in Figs. 4a and 4b, is due to spatial anisotropy under the conditions of a narrow planar pore. Spatial limitations along the pore and across it offer different conditions for growth of chain structures with the "nose to tail" orientation of dipole moments of molecules ($\rightarrow\rightarrow\rightarrow$). Spatial correlations of this type enhance the probability of fluctuation formation of configurations with high dipole moment values and facilitate polarization in the external electric field. There are no hindrances to development of spatial correlations of this type in the direction along the pore plane on the wall side, while the walls confine chain growth in the transverse direction, which results in a decrease in polarizability.

Thus, the main cause of anisotropy of electric properties of an ion–hydrate cluster under the planar pore conditions is suppression of orientation correlation between molecules in the transverse direction. Under the conditions of a planar nanopore, collective effects in interaction of molecules make the tensor of electric polarizability very asymmetric: in a diagonalized tensor, its two lateral components exceeds its transverse component by several times. Obviously, the degree of anisotropy of electric properties must depend on the pore width and must decrease with its growth. The characteristic width of this dependence must be about the size of the radius of intermolecular correlations. Anisotropy of electric properties must change synchronously with the variation of the correlation radius at a change in the temperature. As a rule, the correlation radius in molecular liquids grows at a decrease in temperature. Therefore, one should expect enhancement of anisotropy of electric properties when the system is cooled and it is eliminated under strong heating together with other collective in the system.

3. CONCLUSIONS

Despite the great differences in the energy characteristics, especially in the first reactions of addition of vapor molecules, electric differences of the ion–hydrate complex containing a Na^+ cation under the conditions of a planar nanopore behave qualitatively similarly to the corresponding characteristics of the complex based on the Cl^- anion. In both cases, the growing hydrate shell causes a nonmonotonous variation of the lateral specific electric polarizability that passes through a maximum. An increase in polarizability is due to development of intermolecular orientation correlations at the initial hydration stage and its decrease in the further stages is due to the filling of the space between the ion and the pore wall, where the most rigid orientational order is realized. Strong anisotropy of electric properties of the system is explained by 3D intermolecular correlations promoting formation of chain structures. Nonuniform conditions of development of these correlations in the lateral and transverse direction are the main cause of anisotropy of electric polarizability of the system. Hydrophilic walls adsorb a part of the ion hydrate shell, as a result of which monomolecular film spots are formed on the walls and grow being kept from degradation by the electric field of the ion. In parallel to the spots, "residues" of the hydrate shell not adsorbed on the walls are located at the contact distances from the ion. At the further hydration stages, the gap between the ion and walls is filled by molecules. The pattern of successive growth of different molecular cluster regions is reflected in a nonmonotonous behavior of electric polarizability of the system.

Enhancement of electric polarizability at the initial hydration stages is also promoted by the effect of ion displacement from its own hydrate shell. Forces displacing the ion to the cluster surface cause an increase in the overall dipole moment of the system and thus induce its ability to be polarized in the external field. As displacement of the ion in the confined nanopore space occurs in the direction along the pore plane, the polarizability of the system increases in the same direction. This factor, alongside with intermolecular chain–type correlations promotes enhancement of spatial anisotropy of electric properties of the complex.

The data of computer modeling allowed elucidating the relationship between the 3D organization of the ion–hydrate complex and its electric properties. The obtained results show that the defining role here is played by multiparticle spatial correlations. Despite the strong electric field of the ion, 3D organization of the molecular clot at the room temperatures is far from a geometrically regular crystal structure and is rather closer to a disordered liquid–type structure. Thermal fluctuations and the entropy factor are the key factors under these conditions.

ACKNOWLEDGMENTS

The work was supported by the Russian Foundation for Basic Research (project no. 13-03-00062_a).

REFERENCES

1. New, K.H., Langford, S.C., and Dickinson, J.T., *Appl. Surf. Sci.,* 2002, vol. 197, p. 83.
2. Asencio, R.A., Sababi, M., Pan, J., Ejnermark, S., Ekman, L., and Rutland, M.W., *Corros. Sci.,* 2014, vol. 89, p. 236.
3. Doyle, D.A., Cabral, J.M., Pfuetzner, R.A., Kuo, A., Gulbis, J.M., Cohen, S.L., and Chait, B.T., MacKinnon, R., *Science,* 1998, vol. 280, p. 69.
4. Bakhanova, R.A., Kuku, E.I., Silaev, A.V., Tovstenko, L.M., and Khusid, S.V., *Trudy Vsesoyuz. konf. "Aktivnye vozdeistviya na gidrometeorologicheskie protsessy", Nal'chik, 22-25 oktyabrya 1991 g. Ch. 2* (Proceedings of All-Union Conference "Active Impact on Hydrometeorological Processes," Nalchik,

October 22–25, 1991, Chapter 2), St. Petersburg: Gidrometeoizdat, 1995, p. 218.
5. Scrosati, B., *Nature Nanotechnol.,* 2007, vol. 2, p. 598.
6. Hu, Y.-Sh., Guo, Y.-G., Sigle, W., Hore, S., Balaya, P., and Maier, J., *Nature Mater.,* 2006, vol. 5, p. 713.
7. Chan, C.K., Peng, H., Liu, G., McIlwrath, K., Zhang, X.F., Huggins, R.A., and Cui, Y., *Nature Nanotechnol.,* 2008, vol. 3, p. 31.
8. Grigoriev, S.A., Fedotov, A.A., Fateev, V.N., and Martemianov, S.A., *Russ. J. Electrochem.,* 2016, vol. 52, p. 714.
9. Simon, P. and Gogotsi, Y., *Nature Mater.,* 2008, vol. 7, p. 845.
10. Brezesinski, T., Wang, J., Tolbert, S.H., and Dunn, B., *Nature Mater.,* 2010, vol. 9, p. 146.
11. Ponomarenko, I.V., Parfenov, V.A., Solyanikova, A.S., Chayka, M.Yu., Kravchenko, T.A., and Kirik, S.D., *Russ. J. Electrochem.,* 2015, vol. 51, p. 764.
12. Li, G.V., Astrova, E.V., Rumyantsev, A.M., Voronkov, V.B., Parfen'eva, A.V., Tolmachev, V.A., Kulova, T.L., and Skudin, A.M., *Russ. J. Electrochem.,* 2015, vol. 51, p. 899.
13. Arico, A.S., Bruce, P., Scrosati, B., Tarascon, J.-M., and van Schalkwijk, W., *Nature Mater.,* 2005, vol. 4, p. 366.
14. Maier, J., *Nature Mater.,* 2005, vol. 4, p. 805.
15. Chirkov, Y.G. and Rostokin, V.I., *Russ. J. Electrochem.,* 2014, vol. 50, p. 208.
16. Zamalin, V.M., Norman, G.E., and Filinov, V.S., *Metod Monte-Karlo v statisticheskoi termodinamike (Monte Carlo Method in Statistical Thermodynamics)*, Moscow: Nauka, 1977.
17. Shevkunov, S.V., *Colloid J.,* 2014, vol. 76, p. 490.
18. Shevkunov, S.V., *Russ. J. Electrochem.,* 2014, vol. 50, p. 1118.
19. Shevkunov, S.V., *Russ. J. Electrochem.,* 2014, vol. 50, p. 1127.
20. Shevkunov, S.V., *Russ. J. Phys. Chem. A,* 2014, vol. 88, p. 1744.
21. Shevkunov, S.V., *Russ. J. Phys. Chem. A,* 2014, vol. 88, p. 2165.
22. Shevkunov, S.V., *Russ. J. Electrochem.,* 2016, vol. 52 (in press).
23. Shevkunov, S.V., *Colloid J.,* 2010, vol. 72, p. 93.
24. Shevkunov, S.V., *Russ. J. Electrochem*, 2013, vol. 49, p. 228.
25. Shevkunov, S.V., *Russ. J. Electrochem*, 2013, vol. 49, p. 266.
26. Shevkunov, S.V., *Colloid J.,* 2010, vol. 72, p.107.
27. Shevkunov, S.V., *Colloid J.,* 2011, vol. 73, p. 135.
28. Shevkunov, S.V., *J. Exp. Theor. Phys.,* 2009, vol. 108, p. 2009.
29. Shevkunov, S.V., *Colloid J.,* 2005, vol. 67, p. 509.
30. Shevkunov, S.V., *Russ. J. Phys. Chem.,* 2004, vol. 78, p. 1590.
31. Arshadi, M., Yamdagni, R., and Kebarle, P., *J. Phys. Chem.,* 1970, vol. 74, p. 1466.
32. Olleta, A.C., Lee, H.M., and Kim, K.S., *J. Chem. Phys.,* 2006, vol. 124, p. 024321.
33. Hiroaka, K., Mizuse, S., and Yamade, S., *J. Phys. Chem.,* 1988, vol. 92, p. 3943.
34. Shevkunov, S.V., *Colloid J.,* 2011, vol. 73, p. 275.
35. Shevkunov, S.V., *Colloid J.,* 2009, vol. 71, p. 406.
36. Shevkunov, S.V., *Russ. J. Phys. Chem. A,* 2011, vol. 85, p. 1584.
37. Shevkunov, S.V., *Dokl. Phys.,* 2013, vol. 58, p. 121.
38. Shevkunov, S.V., *Colloid J.,* 2013, vol. 75, p. 444.
39. Burnham, C.J., Petersen, M.K., Day, T.J.F., Iyengar, S.S., and Voth, G.A., *J. Chem. Phys.,* 2006, vol. 124, p. 024327.
40. Herce, D.H., Perera, L., Darden, T.A., and Sagui, C., *J. Chem. Phys.,* 2005, vol. 122, p. 024513.
41. Yoo, S., Lei, Y.A., and Zeng, X.C., *J. Chem. Phys.,* 2003, vol. 119, p. 6083.
42. Shevkunov, S.V., *Colloid J.,* 2008, vol. 70, p. 784.
43. Shevkunov, S.V., *Russ. J. Phys. Chem. A,* 2009, vol. 83, p. 972.
44. Shevkunov, S.V., *High Energy Chem.,* 2009, vol. 43, p. 341.
45. Shevkunov, S.V., *High Energy Chem.*, 2008, vol. 42, p. 205.
46. Hill, T.L., *Statistical Mechanics: Principles and Selected Applications,* Courier Corporation, 1956.

Translated by M. Ehrenburg